SUPPLEMENTAL DATA

Melanocortin 1 Receptor Deficiency Promotes Atherosclerosis in Apolipoprotein E $^{-/-}$ Mice

Petteri Rinne, James J. Kadiri, Mauricio Velasco-Delgado, Salla Nuutinen, Miro Viitala, Maija Hollmén, Martina Rami, Eriika Savontaus, and Sabine Steffens

Correspondence: Petteri Rinne, Institute of Biomedicine, University of Turku, Kiinamyllynkatu 10, 20520 Turku, Finland.
Phone: +358-2-333-7605, Fax: +358-2-333-7216, E-mail: pperin@utu.fi

Supplemental Table I. Quantitative RT-PCR primers for mouse genes.

Gene name Accession number	**5'-3' primer sequence**
ABCA1 NM_013454.3	Forward: gcagatcaagcatcccaact Reverse: ccagagaatgtttcattgtcca
ABCG1 NM_009593.2	Forward: gggtctgaactgccctacct Reverse: tactcccctgatgccacttc
ABCG5 NM_031884.2	Forward: tggatccaacacctctatgctaaa Reverse: ggcaggttttctcgatgaactg
ABCG8 NM_026180.3	Forward: tgcccaccttccacatgtc Reverse: atgaagccggcagtaaggtaga
ACTA2 NM_007392.3	Forward: agattgtgcgcgacatcaaag Reverse: gcagactccataccgataaagga
ACTB NM_007393.5	Forward: tccatcatgaagtgtgacgt Reverse: gagcaatgatcttgatcttca
BAAT NM_007519.3	Forward: tagagcacaccacgttcctg Reverse: gcacaggctcatcaacaaga
BAL (Slc27a5) NM_009512.2	Forward: tgtgtgtgaaggaacctgga Reverse: acccggacaactttgtgaag
BSEP NM_021022.3	Forward: aagctacatctgccttagacacagaa Reverse: caatacaggtccgaccctctct
CCR2 NM_009915.2	Forward: agagagctgcagcaaaaagg Reverse: ggaaagaggcagttgcaaag
CCR5 NM_009917.5	Forward: gagacatccgttccccctac Reverse: gtcggaactgacccttgaaa
COL1A1 NM_007742.4	Forward: gctcctcttaggggccact Reverse: ccacgtctcaccattgggg
COL1A2 NM_007743.3	Forward: tgcagtaacttcgtgcctagc Reverse: acgtggtcctctgtctcca
COL3A1 NM_009930.2	Forward: ctaaaattctgccaccccgaa Reverse: aggatcaacccagtattctccactc
COL4A1 NM_009931.2	Forward: ctggcacaaaagggacgag Reverse: acgtggccgagaatttcacc
CD36 NM_001159558.1	Forward: ccaagctattgcgacatgatt Reverse: tctcaatgtccgagacttttca
CD62P NM_011347.2	Forward: gagggaagaaagccagacg Reverse: ggcgtccaggaacctttt
CX3CR1 NM_009987.4	Forward: cagcatcgaccggtacctt Reverse: gctgcactgtccggttgtt

Gene name Accession number	**5'-3' primer sequence**
CYP7A1 NM_007824.2	Forward: gatcctctgggcatctcaag Reverse: agaggctgctttcattgctt
CYP7B1 NM_007825.4	Forward: gaaaactcttcaaaggcaacatgg Reverse: actggaaagggttcagaacaaatg
CYP8B1 NM_010012.3	Forward: gccttcaagtatgatcggttcct Reverse: gatcttcttgcccgacttgtaga
CYP27A1 NM_024264.5	Forward: gcctcacctatgggatcttca Reverse: tcaaagcctgacgcagatg
DHCR7 NM_007856.2	Forward: gaggcgtccaagaaggtg Reverse: gcagcccattcacctcatac
FXR NM_001163700.1	Forward: tccggacattcaaccatcac Reverse: tcactgcacatcccagatctc
HMGCR NM_008255.2	Forward: tgattggagttggcaccat Reverse: tggccaacactgacatgc
HNF4a NM_008261.3	Forward: accaagaggtccatggtgttt Reverse: gtgccgagggacgatgtag
ICAM1 NM_010493.3	Forward: tggccctggtcaccgttgtgat Reverse: aacagttcacctgcacggaccca
LDLR NM_010700.3	Forward: gcgtaaagaggaggacactgtt Reverse: ccaatctgtccagtacatgaagc
LRH-1 NM_030676.3	Forward: tgggaaggaagggacaatctt Reverse: cgagactcaggaggttgttgaa
LXRα NM_013839.4	Forward: tgggatgtccacgagtgactgttt Reverse: tcccttaatgctacggaaggctct
NTCP NM_011387.2	Forward: gaagtccaaaaggccacactatgt Reverse: acagccacagagagggagaaag
PECAM1 NM_008816.3	Forward: cggtgttcagcgagatcc Reverse: actcgacaggatggaaatcac
S29 NM_009093.2	Forward: atgggtcaccagcagctcta Reverse: agcctatgtccttcgcgtact
SR-A NM_031195.2	Forward: gggagtgtaggcggatca Reverse: tcacagattgtgccccact
SR-BI NM_016741.2	Forward: gcccatcatctgccaact Reverse: tcctgggagccctttttact
SREBP-2 NM_033218.1	Forward: ccaaagaaggagagaggcgg Reverse: cgccagacttgtgcatcttg
VCAM1 NM_011693.3	Forward: ggtcttgggagcctcaacggt Reverse: agggccatggagtcaccgattt

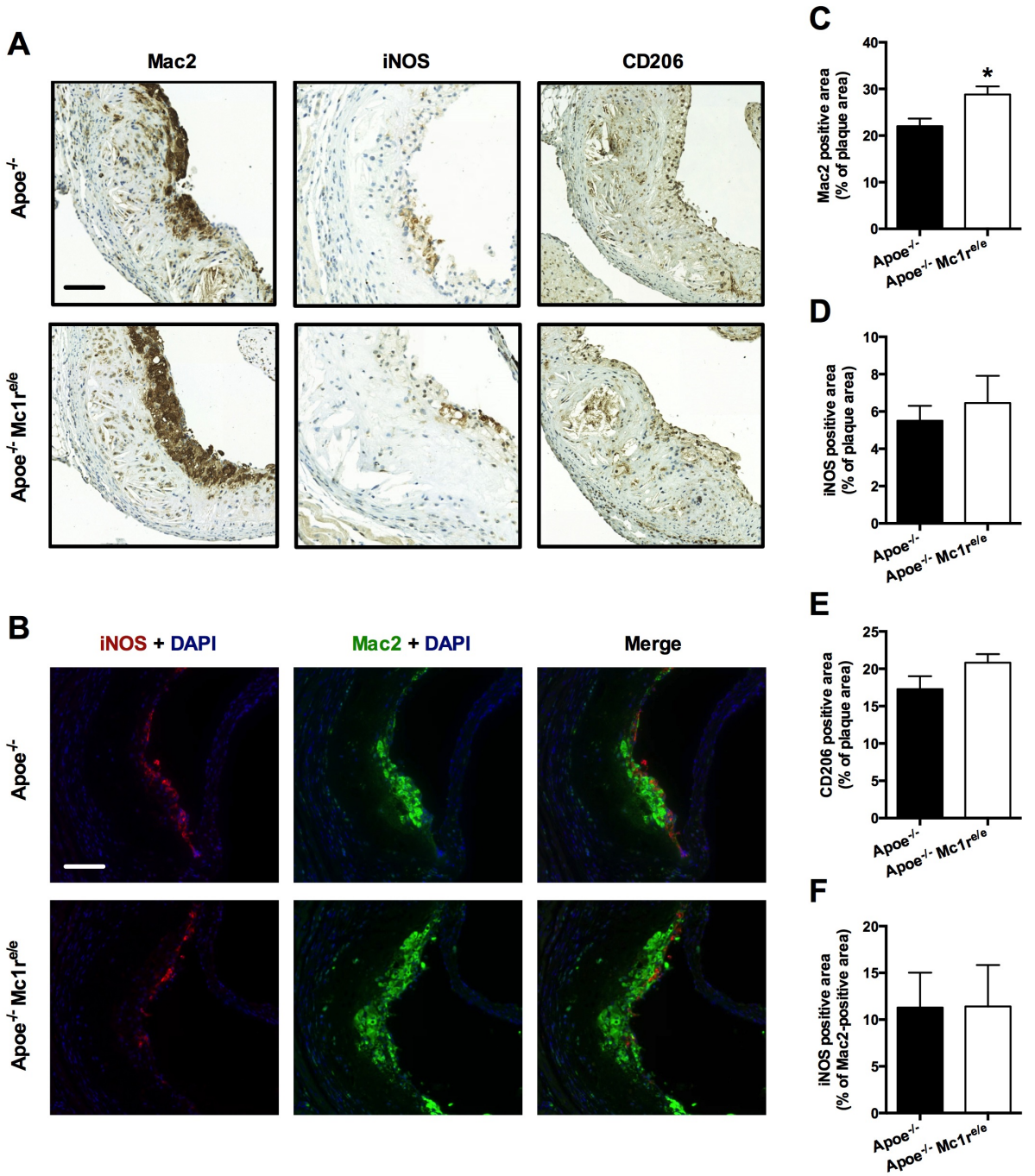

Supplemental Figure I. Melanocortin 1 receptor deficiency enhances macrophage content in aortic plaques of high-fat diet (HFD)-fed Apoe$^{-/-}$ mice without affecting macrophage polarization. **A,** Representative images of Mac2, iNOS and CD206 immunostaining of the aortic sinus of Apoe$^{-/-}$ and Apoe$^{-/-}$ Mc1r$^{e/e}$ mice fed a high-fat diet (HFD) for 12 wks. Scale bar, 100 µm. **B**, Representative immunofluorescent stainings of iNOS and Mac2 in the aortic roots of HFD-fed Apoe$^{-/-}$ and Apoe$^{-/-}$ Mc1r$^{e/e}$ mice. Scale bar, 100 µm. **C** through **F**, Quantification of Mac2-, iNOS- and CD206 positive areas (expressed as % of plaque area) as well as iNOS-positive macrophage area (% of Mac2-positive area) in the aortic sinuses. n=5-10 mice per group in each graph. * P<0.05 versus Apoe$^{-/-}$ mice by Student's t-test. Values are mean ± SEM.

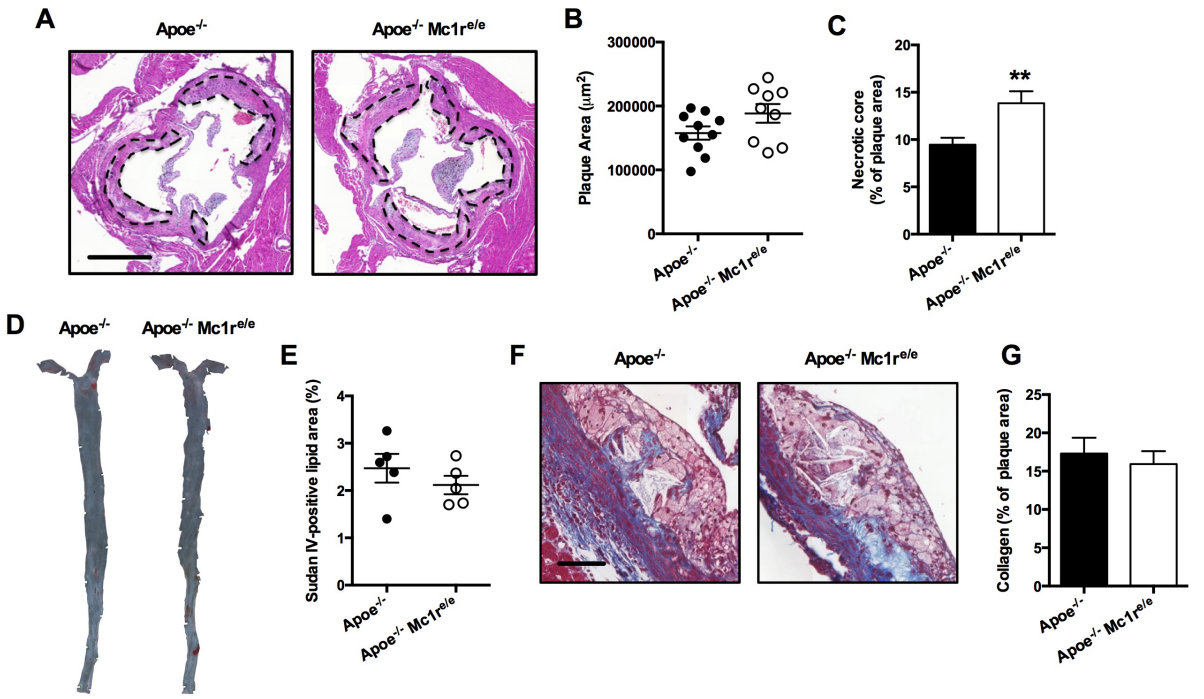

Supplemental Figure II. Atherosclerotic plaque size and composition in chow-fed Apoe$^{-/-}$ and Apoe$^{-/-}$ Mc1r$^{e/e}$ mice. A, Representative images of hematoxylin and eosin (H&E) staining of the aortic sinus of Apoe$^{-/-}$ and Apoe$^{-/-}$ Mc1r$^{e/e}$ mice fed a normal chow diet. Mice were euthanized at the age of 6 months and were age-matched with the 12 wks HFD mice. Scale bar, 500 µm. **B**, Quantification of plaque area in aortic sinuses. **C**, Quantification of acellular necrotic core areas as percentage of total plaque area. **D** and **E**, Representative en face Sudan IV stainings and quantification of Sudan IV-positive lipid area in the aorta. **F**, Representative images of Masson's trichrome staining in the aortic sinus. **G**, Quantification of plaque collagen content as percentage of total plaque area. Scale bar, 100 µm. n=8-10 mice per group in each graph, except for E (n=5 per group). ** P<0.01 versus Apoe$^{-/-}$ mice by Student's t-test. Values are mean ± SEM.

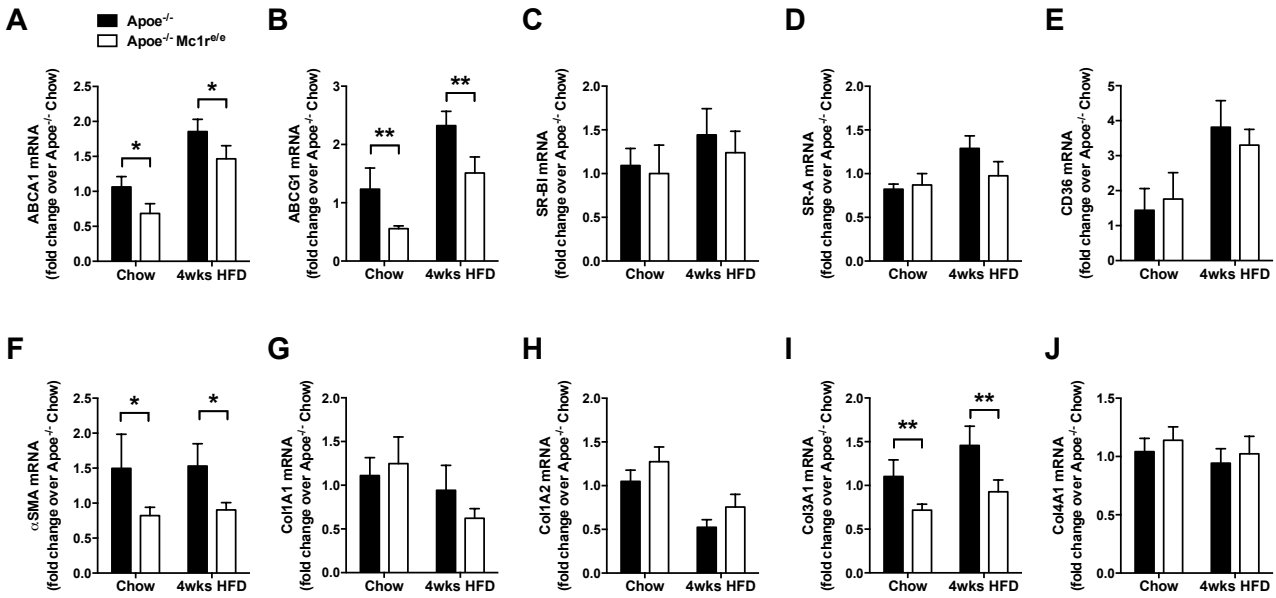

Supplemental Figure III. Expression of cholesterol transport and stability-related genes in the aorta of Apoe$^{-/-}$ and Apoe$^{-/-}$ Mc1r$^{e/e}$ mice. Quantitative RT-PCR analysis of the indicated genes in the aorta of Apoe$^{-/-}$ and Apoe$^{-/-}$ Mc1r$^{e/e}$ mice fed a normal chow diet or high-fat diet (HFD) for 4 weeks. **A**, ABCA1, ATP-binding cassette sub-family A member 1. **B**, ABCG1, ATP-binding cassette sub-family G member 1. **C**, SR-BI, scavenger receptor class B member 1. **D**, SR-A, macrophage scavenger receptor 1.**E**, CD36, scavenger receptor class B member 3. **F**, αSMA, alpha smooth muscle actin. **G** through **J**, Collagen, type I, alpha 1 (Col1A1) and alpha 2 (Col1A2), type III, alpha 1 (Col3A1) and type IV, alpha 1 (Col4A1). * P<0.05 and ** P<0.01 for genotype effect by 2-way ANOVA. Interaction between the genotype and diet as well as pairwise comparisons within diet groups by Bonferroni *post hoc* tests were non-significant. Data are mean ± SEM, n=7-8 mice per group.

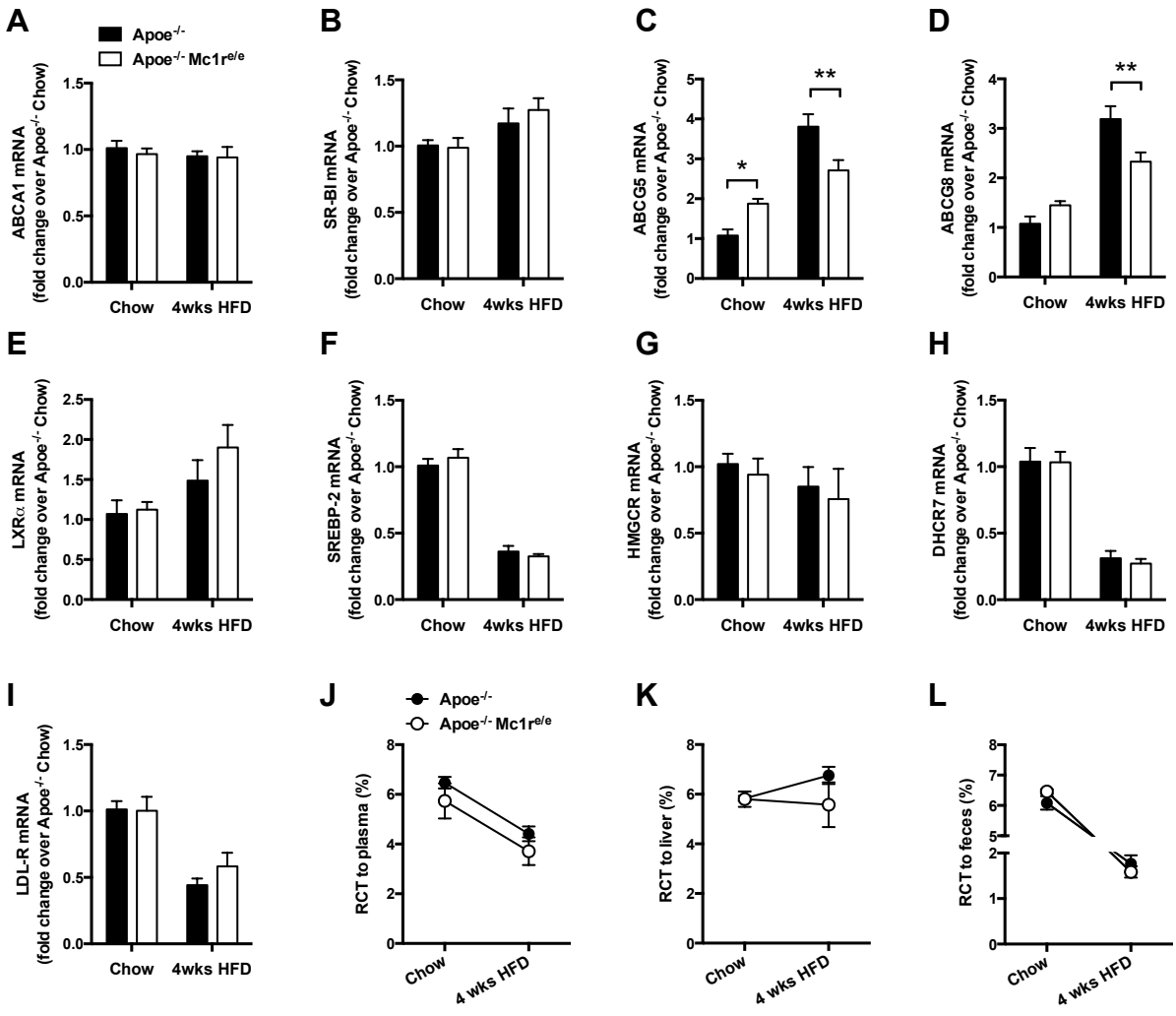

Supplemental Figure IV. Hepatic expression of cholesterol transport and synthesis genes in Apoe$^{-/-}$ and Apoe$^{-/-}$ Mc1r$^{e/e}$ mice. Quantitative RT-PCR analysis of genes involved in cholesterol transport and synthesis in the liver of Apoe$^{-/-}$ and Apoe$^{-/-}$ Mc1r$^{e/e}$ mice fed a normal chow diet or high-fat diet (HFD) for 4 weeks. **A**, ABCA1, ATP-binding cassette sub-family A member 1. **B**, SR-BI, scavenger receptor class B member 1. **C**, ABCG5, ATP-binding cassette sub-family G member 5. **D**, ABCG8, ATP-binding cassette sub-family G member 8. **E**, LXRα, liver X receptor alpha. **F**, SREBP-2, sterol regulatory element-binding protein 2. **G**, HMGCR, HMG-CoA reductase. **H**, DHCR7, 7-dehydrocholesterol reductase. **I**, LDL-R, low-density lipoprotein receptor. n=8 mice per group. **J** through **L**, Plasma, liver and fecal radioactivities at 48 hours after injection of ^{3}H-cholesterol-labelled macrophages. Data are expressed as percentage of total injected ^{3}H-radioactivity. Samples for chow and 4 wks HFD groups were derived from different sets of mice. n=4-6 mice per group. * P<0.05 and ** P<0.01 versus Apoe$^{-/-}$ mice by 2-way ANOVA and Bonferroni *post hoc* tests. Data are mean ± SEM, n=7-10 per group.

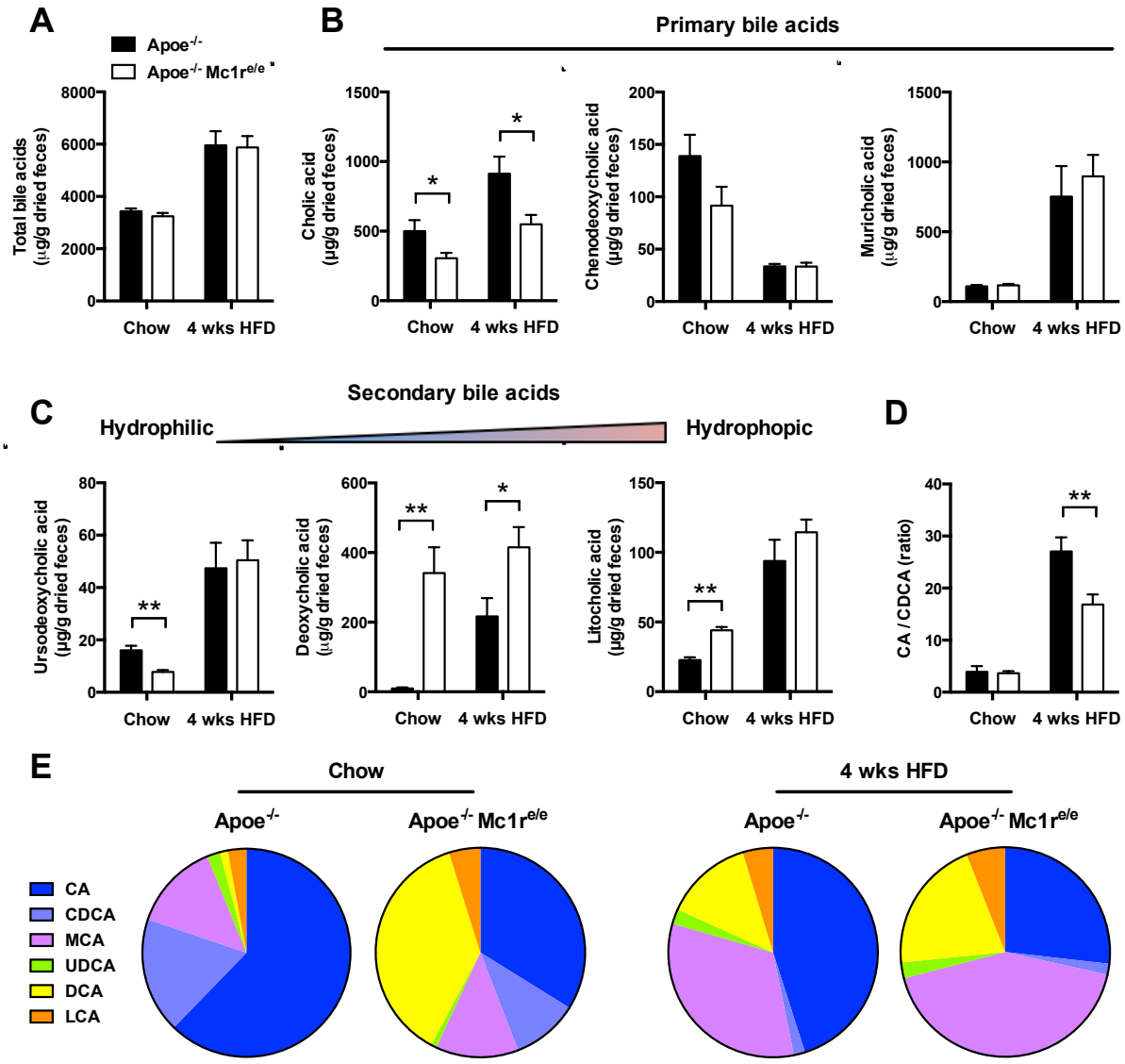

Supplemental Figure V. Composition of the fecal bile acid pool in Apoe$^{-/-}$ and Apoe$^{-/-}$ Mc1r$^{e/e}$ mice. Feces were collected over 48 h and quantified for total bile acids (**A**), the primary bile acids; cholic acid, chenodeoxycholic acid and murocholic acid (**B**), and the secondary bile acids; ursodeoxycholic acid, deoxycholic acid and litocholic acid (**C**). The results are presented as µg per g of dried feces. **D**, The ratio of cholic acid to chenodeoxycholic acid was calculated as a measure of bile acid hydrophilicity. **E**, Relative distribution of individual bile acids in the fecal samples of Apoe$^{-/-}$ and Apoe$^{-/-}$ Mc1r$^{e/e}$ mice. CA, cholic acid; CDCA, chenodeoxycholic acid; MCA, muricholic acid; UDCA, ursodeoxycholic acid; DCA, deoxycholic acid; LCA, litocholic acid,. * P<0.05 and ** P<0.01 versus Apoe$^{-/-}$ mice by 2-way ANOVA and Bonferroni *post hoc* tests. Data are mean ± SEM, n=4-6 mice per group.

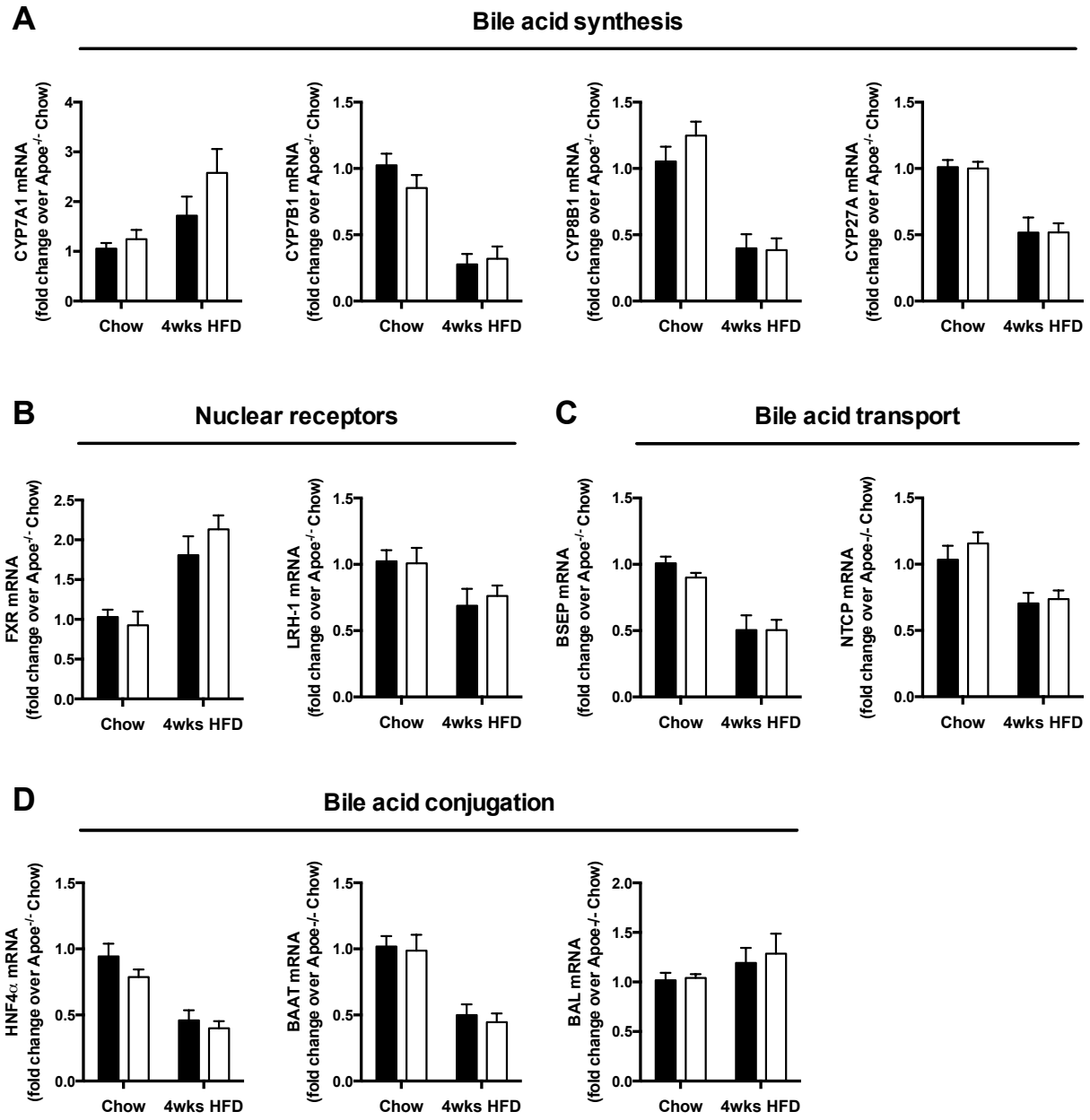

Supplemental Figure VI. Hepatic expression of genes that govern bile acid synthesis, transport and conjugation. Quantitative RT-PCR analysis of genes involved in the bile acid synthesis (**A**), transport (**B**) and conjugation (**C**) in the liver of Apoe$^{-/-}$ and Apoe$^{-/-}$ Mc1r$^{e/e}$ mice fed a normal chow diet or high-fat diet (HFD) for 4 weeks. CYP7A1, cholesterol 7 alpha-hydroxylase; CYP7B1, 25-hydroxycholesterol 7-alpha-hydroxylase; CYP8B1, sterol 12-alpha-hydroxylase; CYP27A1, sterol 27-hydroxylase; FXR, farnesoid X receptor; LRH-1, liver receptor homologue 1; BSEP, bile-salt export pump; NTCP, Na+-taurocholate cotransporting polypeptide; HNF4α, hepatocyte nuclear factor 4 alpha; BAAT, bile acid-CoA:amino acid N-acyltransferase; BAL, bile acid-CoA ligase. * $P<0.05$ and ** $P<0.01$ versus Apoe$^{-/-}$ mice by 2-way ANOVA and Bonferroni *post hoc* tests. Data are mean ± SEM, n=8 mice per group.

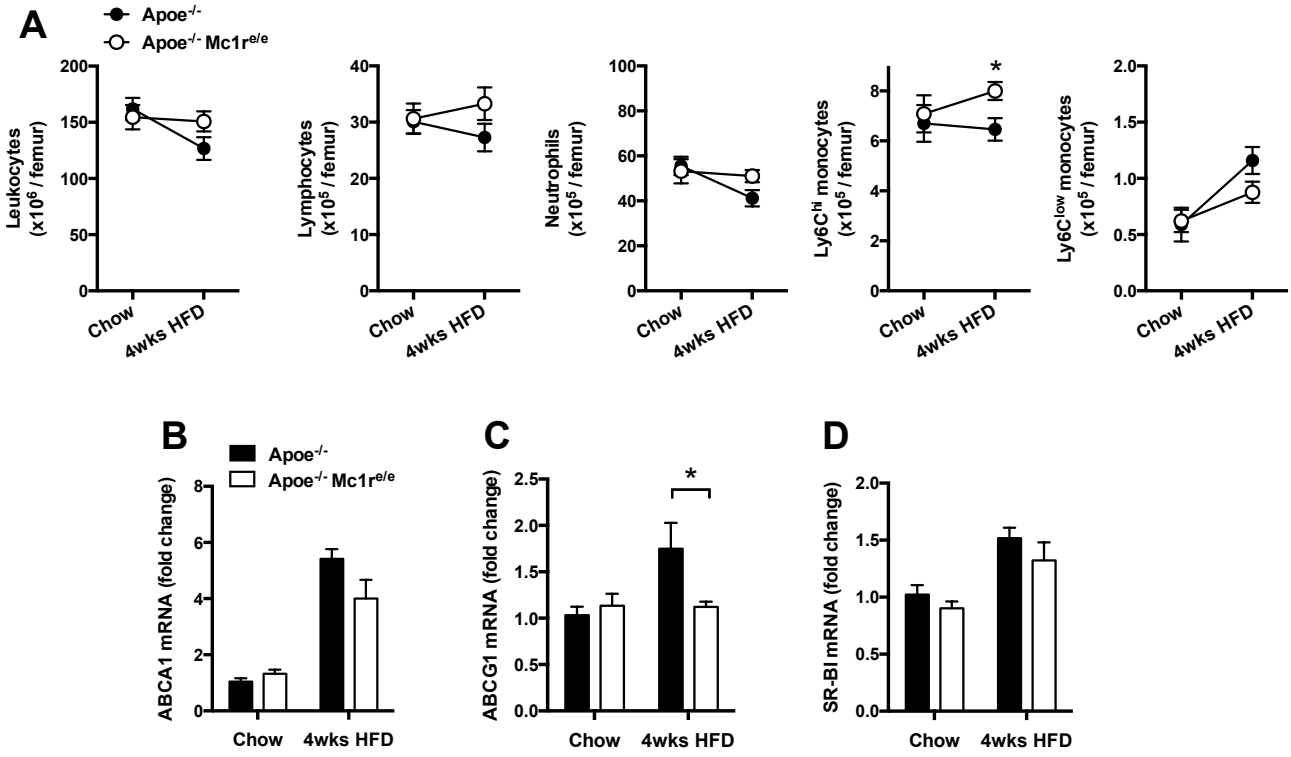

Supplemental Figure VII. Melanocortin 1 receptor deficiency accelerates monocytosis in HFD-fed Apoe$^{-/-}$ mice. A, Quantification of total leukocytes (CD45^{+}), lymphocytes (CD45^{+}, CD11b^{-}), neutrophils (CD45^{+}, CD11b^{+}, Ly6G), Ly6C^{high} monocytes (CD45^{+}, CD11b^{+}, CD115^{+}, Ly6C^{high}) and Ly6C^{low} monocytes (CD45^{+}, CD11b^{+}, CD115^{+}, Ly6C^{low}) in the bone marrow of Apoe$^{-/-}$ mice and Apoe$^{-/-}$ Mc1r$^{e/e}$ mice fed a normal chow diet or high-fat diet (HFD) for 4 weeks. Samples for chow and 4 wks HFD groups were derived from different sets of mice. **B**, Quantitative RT-PCR analysis of ATP-binding cassette transporter A1 (ABCA1), G1 (ABCG1) and scavenger receptor class B member 1 (SR-BI) expression in the bone marrow of Apoe$^{-/-}$ mice and Apoe$^{-/-}$ Mc1r$^{e/e}$ mice. * P<0.05 versus Apoe$^{-/-}$ mice by 2-way ANOVA and Bonferroni *post hoc* tests. Data are mean ± SEM, n=7-10 per group.

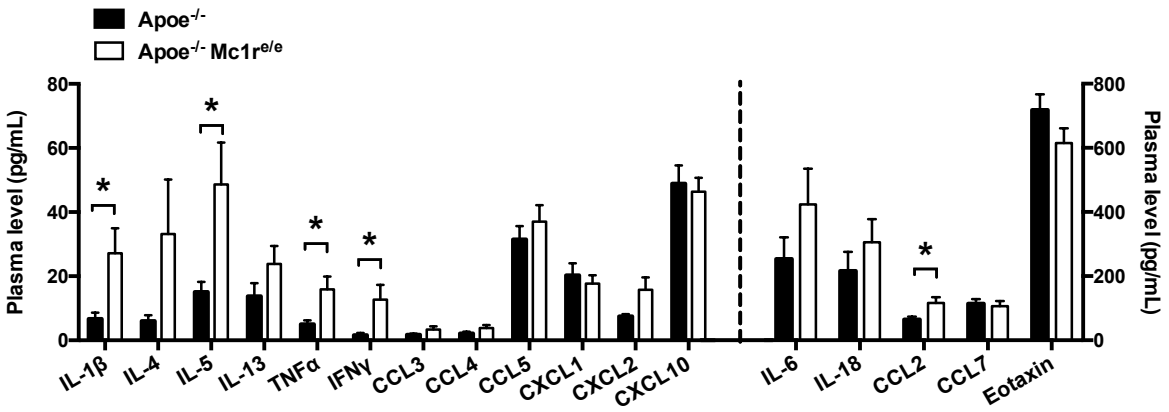

Supplemental Figure VIII. Melanocortin 1 receptor deficiency elevates pro-inflammatory cytokine levels in chow-fed Apoe$^{-/-}$ mice. Plasma cytokine levels in chow-fed Apoe$^{-/-}$ and Apoe$^{-/-}$ Mc1r$^{e/e}$ mice. * P<0.05 versus Apoe$^{-/-}$ mice by Student's t test. Data are mean ± SEM, n=12-13 per group.

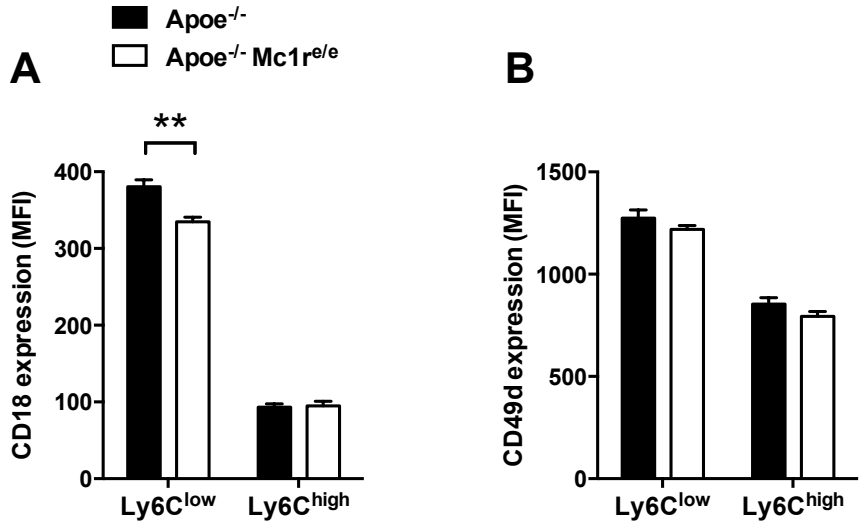

Supplemental Figure IX. Integrin expression in blood monocytes from chow-fed Apoe$^{-/-}$ mice. Mean fluorescence intensity (MFI) of CD18 (**A**) and CD49d (**B**) in the Ly6C^{low} and Ly6C^{high}-gated blood monocytes from chow-fed Apoe$^{-/-}$ and Apoe$^{-/-}$ Mc1r$^{e/e}$ mice. ** P<0.01 versus Apoe$^{-/-}$ mice by 2-way ANOVA and Bonferroni *post hoc* tests. Data are mean ± SEM, n=8 mice per group.

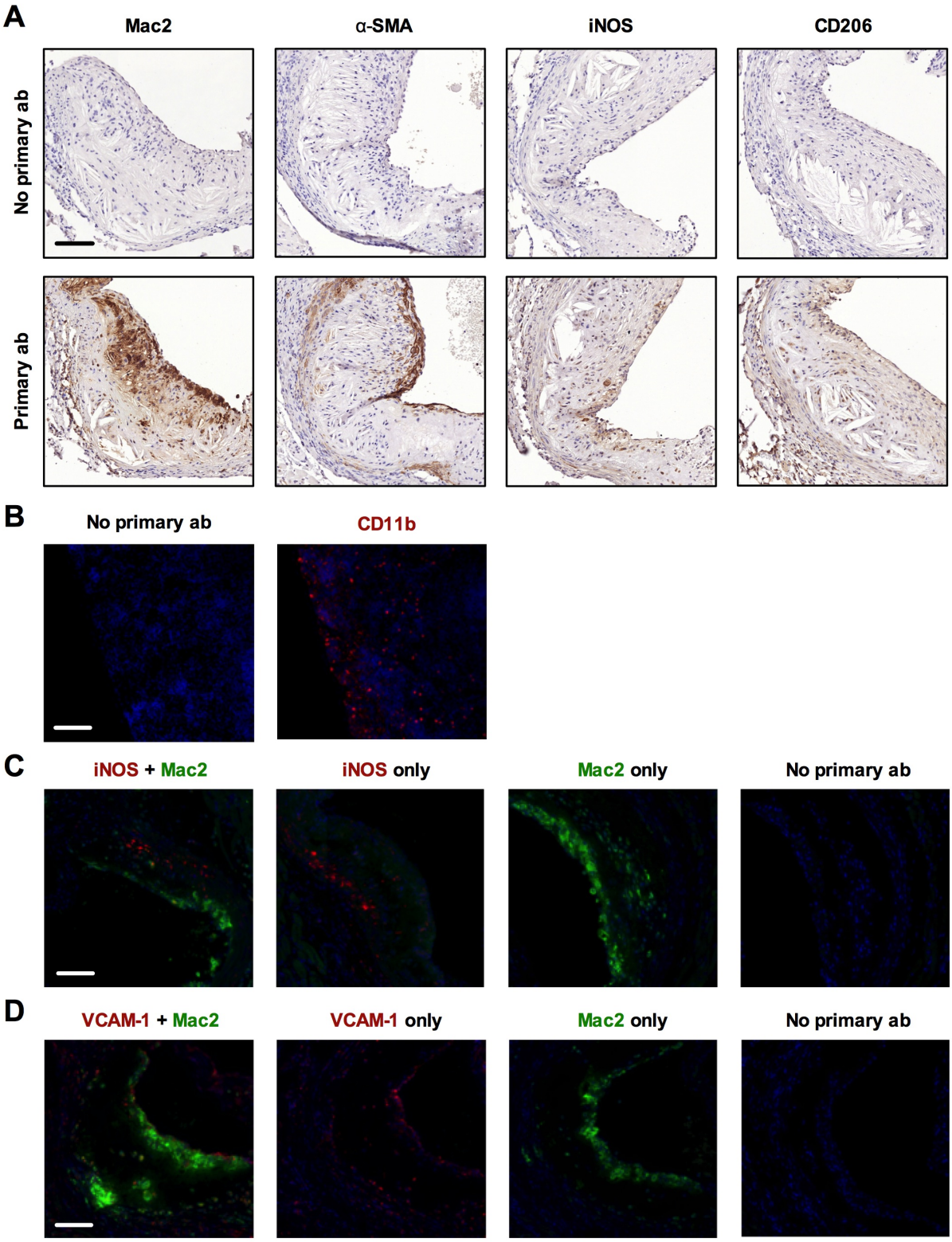

Supplemental Figure X. Controls for immunohistochemistry and immunofluorescence. Negative controls for Mac2, α-SMA, iNOS and CD206 (**A**) and CD11b (**B**) were obtained by staining consecutive sections with the appropriate secondary antibodies only. **C-D**, Appropriate single stain and no primary antibody controls are presented for iNOS+Mac2 and VCAM-1+Mac2 immunofluorescence staining. Scale bar, 100 μm in each panel.